

## Predicting the enhancement of mixing-driven reactions in nonuniform flows using measures of flow topology

Nicholas B. Engdahl

*Department of Civil and Environmental Engineering, Washington State University, Pullman, Washington 99164, USA*

David A. Benson

*Hydrologic Science and Engineering, Colorado School of Mines, Golden, Colorado 80401, USA*

Diogo Bolster

*Department of Civil and Environmental Engineering and Earth Sciences, University of Notre Dame, Notre Dame, Indiana 46556, USA*

(Received 7 February 2014; published 13 November 2014)

The ability for reactive constituents to mix is often the key limiting factor for the completion of reactions across a huge range of scales in a variety of media. In flowing systems, deformation and shear enhance mixing by bringing constituents into closer proximity, thus increasing reaction potential. Accurately quantifying this enhanced mixing is key to predicting reactions and typically is done by observing or simulating scalar transport. To eliminate this computationally expensive step, we use a Lagrangian stochastic framework to derive the enhancement to reaction potential by calculating the collocation probability of particle pairs in a heterogeneous flow field accounting for deformations. We relate the enhanced reaction potential to three well known flow topology metrics and demonstrate that it is best correlated to (and asymptotically linear with) one: the largest eigenvalue of the (right) Cauchy-Green tensor.

DOI: [10.1103/PhysRevE.90.051001](https://doi.org/10.1103/PhysRevE.90.051001)

PACS number(s): 47.56.+r, 47.51.+a, 47.85.lk

Mixing-driven reactions are ubiquitous in physical systems because they represent the general process where two or more species come into contact and with some probability, or rate, produce something different. While many studies relate specifically to chemical reactions across a wide range of scales within different media including carbon nanotubes [1], porous media [2], intracellular biochemistry [3], and atmospheric flows [4], to name a few, the principles have broad application to other disciplines including mathematical biology [5,6], ecology [7], economics [8,9], natural and social sciences [10], and general chemical physics [11]. In all cases, a key feature is that reactions only occur when constituents come into contact; random motions at small scales make this a stochastic process. Thus an accurate representation of contact processes is key to successful prediction of reactions [12]. This is particularly challenging in flowing systems, where heterogeneities in deterministic transport processes can separate or bring reactants into closer proximity.

Inaccuracies in models for the rate at which reactants are brought together via mixing can compound over time, resulting in mismatches between measured and predicted rates of reaction [2,13–15]. Because direct simulation of large-scale transport in nonuniform flows with small-scale reactions is computationally expensive, surrogate relationships between mixing and reactions have been explored using a variety of tools, including metrics based on entropy [16], scalar dissipation rates [17–19], and concentration probability distributions [20,21]. However, none of those studies have shown the exact link between reactions and the fluid deformation that leads to enhanced mixing. Furthermore, quantifying these metrics still requires prior knowledge of scalar transport. This must be obtained numerically or experimentally, which can be costly and difficult to measure adequately for reasons including numerical dispersion or noise [17] and experimental error or resolution [22]. An alternative is to identify reliable measures of reaction

enhancement based directly on the flow field, which is easier to calculate or measure. In this Rapid Communication we derive the relationship between reactions and the underlying flow structure, based on how changes in collocation probabilities can be inferred from the flow's strain field.

*Theory: collocation and reactions.* A growing body of evidence shows that mixing is a primary limiting factor in the progress of reactions across a huge range of scales, from carbon nanotubes to the very early expanding universe [1,13,23–25]. Here we show that the problem can be reduced to calculating the likelihood that reactive particles collocate, which can be quantified by a collocation density (CLD). The importance of mixing is evident in the classical chemical Langevin equation [26] for reactions between sets of perfectly mixed particles. This equation shows that the propensity for a reaction to occur is given by the product of two probabilities: The first is the probability that reacting particles are collocated and the second is the thermodynamic probability that a reaction will happen, given collocation. Perfect mixing assumes that the collocation probability is uniform for all particle combinations. We can generalize this classical picture by considering the true collocation probabilities for particle combinations [27–29]. Over a finite-time interval  $\Delta t$ , a bimolecular reaction will occur with probability

$$P(\mathbf{s}|\Delta t) = \xi v(\mathbf{s})d\mathbf{s}, \quad (1)$$

where two reactive particles are initially separated by displacement  $\mathbf{s}$ ,  $\xi = m_p k \Delta t$  is the thermodynamic probability, given the well-mixed reaction rate  $k$ , that the reaction occurs given collocation of reactant particles of mass  $m_p$ , and  $v(\mathbf{s})d\mathbf{s}$  is the probability that the particles collocate within  $\Delta t$ . Previous work has shown that (1) is applicable to general reactions and that it recovers the correct continuum scale equations [29–31]. The probability  $\xi$  may be treated as a constant if it is much larger than  $v(\mathbf{s})d\mathbf{s}$ , defining the mixing-limited condition, and

the reaction probability depends most sensitively on and is linear with the CLD  $\nu(\mathbf{s})$ . Estimation of reaction rates is now reduced to calculating the CLD, which has traditionally been done using particle tracking or other numerical techniques.

The CLD is a direct analog for mixing-limited reaction rates for an arbitrary number of constituents, because all reactions are combinations of monomolecular and bimolecular reactions [26]. All particle pairs for any reaction will have some finite CLD and the values of the CLD can be affected significantly by a spatially heterogeneous velocity field. Consider two particles initially separated by displacement  $\mathbf{s}$ . Over a time  $\Delta t$ , these particles will move and their new positions will be described by a set of probability density functions, reflecting both the underlying deterministic and stochastic transport processes. The CLD for this particle pair can be calculated as the convolution of these probability density functions [27–29]. Assuming multi-Gaussian distributions of particle positions, consistent with Fickian transport in  $d$  dimensions [32], the probability density that the two particles will occupy the same position after  $\Delta t$  is

$$\nu(\mathbf{s}) = \frac{1}{\sqrt{(2\pi)^d \det[\kappa_A + \kappa_B]}} \exp\left[-\frac{1}{2} \mathbf{s}^T (\kappa_A + \kappa_B)^{-1} \mathbf{s}\right], \quad (2)$$

where  $\kappa_i$  is the covariance matrix associated with each particle's  $d$ -dimensional motion, which along with diffusion can account for shear, rotation, and dilation and compression [32,33]. Note that (2) can be generalized to non-Fickian transport if anomalous diffusion is observed [34]. The CLD (2) quantifies how changes in proximity  $\mathbf{s}$  or dispersive magnitudes  $\kappa$  lead to changes in reaction probability.

*The CLD and fluid deformation.* A significant benefit of the CLD is that it can be estimated without the need to measure or explicitly simulate transport. Changes in the CLD due to heterogeneous flow can be inferred from the flow's strain field. The Lagrangian deformation-gradient tensor  $\mathbf{F}$  quantifies the sensitivity of a particle's final position to small perturbations in its initial position over a specific interval of time [35]. However, because the changes in position for steady-state incompressible flows are caused by velocity gradients, we write the deformation-gradient tensor for these conditions to leading order using the flow strain tensor  $\mathbf{E} = \nabla \mathbf{u}$  as

$$\mathbf{F}(\mathbf{x}) = \Delta t \mathbf{E} + O(\Delta t^2), \quad (3)$$

where  $\mathbf{u}$  is the velocity vector, which in two dimensions has components  $(u_x, u_y)$ . For small time scales  $\Delta t$ , the first-order approximation of the changes in position is valid. The diagonal terms of  $\mathbf{F}$  may be regarded as dilation and compression and the off-diagonals as shear and/or rotation. The deformation-gradient tensor quantifies how an initially  $d$ -dimensional volume element will be reshaped by the flow field. The significance of  $\mathbf{F}$  is that it is a direct indication of the forces acting on a material element that change the CLD and modify reaction rates. For any incompressible flow, the deformation of a fluid parcel will bring some enclosed particles into closer proximity, directly changing the CLD relative to an equivalent undeformed parcel.

*Traditional flow topology metrics.* Let us consider three other classical flow topology metrics that are often used to study flowing systems in nonuniform velocity fields and com-

pare them to the CLD. The Okubo-Weiss parameter  $\Theta(\mathbf{x}) = -4 \det(\mathbf{E})$  is a common measure of the overall strength of flow deformation [33]. For two-dimensional (2D) incompressible flow,  $\Theta = 4[E_{11}^2 + E_{12}E_{21}]$ , emphasizing the balance between shear, rotation, and dilatation and compression. Another common measure of flow deformation is based on the (right) Cauchy-Green strain tensor, which removes rotation [35]:

$$\mathbf{C}(\mathbf{x}) = [\mathbf{F}]^T \mathbf{F}. \quad (4)$$

The eigenvalues and eigenvectors of  $\mathbf{C}(\mathbf{x})$  give the intensity and direction of the dominant deformations, respectively. For 2D incompressible flow the eigenvectors are orthogonal. The strength of the deformation can be quantified from the largest eigenvalue of  $\mathbf{C}(\mathbf{x})$ , denoted by  $\lambda_C$ . A third common metric for quantifying deformation is the finite-time Lyapunov exponent (FTLE) [36,37], defined by  $\Lambda(\mathbf{x}) = \ln[\lambda_C(\mathbf{x})]/2\Delta t$ . Here we show that these common flow topology measures  $\Theta$ ,  $\lambda_C$ , and  $\Lambda$  can be related (some more directly than others) to changes in reaction rates, because changes in relative particle positions are proportional to the intensity of the local deformations. However, it should be noted that because they are independent of problem-specific initial conditions, the fields of the deformation metrics represent unconditional maps of the potential for reaction rates in mixing-limited systems and represent the maximum possible enhancement that will occur due to deformation. Estimation of actual reaction rates will require integration of the deformation metrics along fluid pathways and consideration of the local arrangement of multiple chemical species.

For a more quantitative link to reaction, we define the local maximum relative change in reaction rate as the ratio of CLD after some motion that may incur deformation (and deformation-related dispersion) to the undeformed (premotion) CLD

$$\nu_E(\mathbf{s}) = \frac{\nu(\mathbf{s})}{\nu(\mathbf{s}_0)}. \quad (5)$$

The ratio  $\nu_E(\mathbf{s})$  quantifies the maximum increase in CLD due to fluid deformation associated with the underlying velocity field relative to a system where no such deformation has occurred. The values of  $\mathbf{s}$  and  $\kappa_i$  in (2) for any particle pair must be estimated before and after a small amount of time to make this calculation. The diffusive properties will change slowly relative to advection over a small time step  $\Delta t$ , consistent with the idea that the system is mixing limited. Therefore, the change in CLD depends primarily on the mean motion of the particles relative to each other, the effect of which is quantified by the velocity gradients. Because rotation does not bring particles in a volume any closer to each other, we use the common decomposition of  $\mathbf{E}$  into strain  $\varepsilon$  and rotation  $\omega$  tensors, respectively (in two dimensions):

$$\mathbf{E} = \varepsilon + \omega = \frac{1}{2} \begin{bmatrix} \alpha & \sigma \\ \sigma & -\alpha \end{bmatrix} + \frac{1}{2} \begin{bmatrix} 0 & -\omega \\ \omega & 0 \end{bmatrix}, \quad (6)$$

where  $\alpha = 2\partial u_x/\partial x$ ,  $\sigma = \partial u_y/\partial x + \partial u_x/\partial y$ , and  $\omega = \partial u_y/\partial x - \partial u_x/\partial y$ . Rather than calculate the potential displacement changes for all particle pairs in a small volume, we use a measure of the maximum changes held in the largest magnitude eigenvalue of the strain matrix  $\varepsilon$  that we denote by  $\lambda_\varepsilon = \frac{1}{2}\sqrt{\alpha^2 + \sigma^2}$ . It can be shown that, to first order, the

change in CLD will be proportional to this eigenvalue, so for small  $\Delta t$ ,

$$\Delta \mathbf{s} = \mathbf{s}_0 - \mathbf{s} \approx \mathbf{s}_0 \Delta t \lambda_\epsilon, \quad (7)$$

where  $\mathbf{s}_0$  is the initial separation vector.

The covariance matrix of dispersion  $\kappa$  is determined from  $\mathbf{E}$  and the local isotropic diffusion coefficient  $D_m$  [32,33]. In the rotation-removed ( $\omega = 0$ ) reference frame,  $\kappa$  has eigenvalues  $\lambda_{\kappa 1}$  and  $\lambda_{\kappa 2}$  given by

$$\lambda_{\kappa 1,2} = \pm \frac{2D_m}{\lambda_\epsilon} [\exp(\pm \lambda_\epsilon \Delta t) - 1]. \quad (8)$$

In the case of uniform or simple rotating flow,  $\lambda_\epsilon \rightarrow 0$  and dispersion is by normal diffusion ( $\lambda_{\kappa 1} = \lambda_{\kappa 2} = 2D_m \Delta t$ ).

With (7) and (8), the changes in CLD can be found by specifying an appropriate time scale  $\Delta t$ , diffusion coefficient  $D_m$ , initial separation distance  $\mathbf{s}_0$ , and the magnitude of the velocity gradients. For steady flow, these calculations are made only once. This approach gives an estimation of the distribution of potential reaction rates within any domain without needing to explicitly simulate transport or reactions.

*A simple example.* Consider 2D flow with compression along the  $x$  axis and no shear so that  $\partial u_x / \partial x = -\alpha$  and  $\partial u_y / \partial y = \alpha$ . Then  $\mathbf{F} = (\Delta t/2) \text{diag}(-\alpha, \alpha)$  and  $\lambda_\epsilon = \alpha/2$ . The CLD after motion is Gaussian with  $\mathbf{s} = \mathbf{s}_0(1 - \Delta t \alpha/2)$  and variances along the  $y$  and  $x$  axes given by (8). The deformation metrics for this example are  $\Theta = \alpha^2$ ,  $\lambda_C = (\Delta t \alpha/2)^2$ , and  $\Lambda = \ln(\Delta t \alpha/4)/\Delta t$ . In this case, the descriptions of the Okubo-Weiss parameter, the FTLE, and the largest eigenvalue of Cauchy-Green tensor are scaled variations of each other because of the simplicity of the assumed flow field, although the FTLE is weighted logarithmically rather than linearly with  $\alpha$ , which highlights a different sensitivity. The change in reactivity  $v_E(\mathbf{s})$  can be calculated for this simple case using (2) in (5), which gives  $v_E = \exp[(-\mathbf{s} \cdot \mathbf{s} + \mathbf{s}_0 \cdot \mathbf{s}_0)/8D_m \Delta t]$ , assuming the changes in  $\mathbf{s}$  overshadow changes in  $\kappa$ . Then choosing a representative separation distance  $s_0$  for the volume, in the small- $\Delta t$  limit the exponential using (7) expands to  $v_E \approx 1 + s_0^2 \Delta t \alpha^2 / 32D_m$ . In a practical sense,  $\Delta t$  and  $D_m$  are fixed values and in this simple compressional regime, the reaction increase is linear with  $\lambda_C$  and  $\Theta$ . As  $\alpha \rightarrow 0$  or  $\kappa \rightarrow \infty$ , there is no reaction enhancement. The former is uniform flow and the latter is already perfectly mixed.

If the gradients of the velocity field from the previous example are rotated  $90^\circ$  so that  $\partial u_x / \partial x = \alpha$  and  $\partial u_y / \partial y = -\alpha$ , this changes the deformation from compression to an extensional regime, but it is trivial to show that  $\lambda_C$ ,  $\Lambda$ , and  $\Theta$  are unchanged by this alteration, as is  $v_E(\mathbf{s})$ . This illustrates that the unconditional CLD (independent of initial conditions) in a heterogeneous velocity field will always be greater than the CLD for diffusion in uniform flow, regardless of the direction of the deformations. In incompressible flow, any extension that separates some particles is balanced by compression normal to the extension that brings other particles together.

*A synthetic heterogeneous example.* The connection between the changes in reaction potential  $v_E(\mathbf{s})$  and the classical deformation metrics is now illustrated using an example of 2D steady flow through a heterogeneous flow field. The field is generated from Darcy flow through a synthetic porous medium with a fractal hydraulic conductivity  $K$ , which varies over five

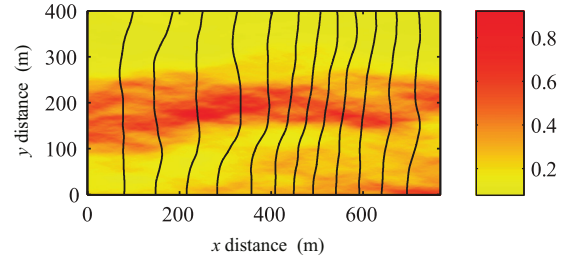


FIG. 1. (Color online) Magnitude of the velocity field and pressure equipotentials (dark solid lines). Flow is from left to right and velocities are in  $m/d$ .

orders of magnitude. Flow is from left to right with no flow at the upper and lower vertical boundaries (Fig. 1). Local Fickian dispersion is modeled with an isotropic dispersion coefficient  $D_m = 0.1 \text{ m}^2/d$ .

The flow topology metrics ( $\Theta$ ,  $\Lambda$ , and  $\lambda_C$ ) and relative CLD  $v_E$  are calculated at each grid point (Figs. 2 and 3). The square root of  $\Theta$  is plotted to improve visual contrast. Recall that in a uniform velocity field with identical diffusion coefficients, by the principle of Galilean invariance, there would be no changes in CLD since all particles would be translated equally and have the same chance for random diffusion and collision. Clearly, all the deformation metrics contain some information about how the velocity field affects the CLD, but  $\Theta$  and FTLE give, respectively, noisy and overly smooth views of the areas that will have the most intense mixing. In contrast,  $\lambda_C$  gives an almost identical rescaled map of the relative changes in CLD and shows areas of up to 40% increased reaction potential due to fluid deformation [Fig. 3(a)].

An analysis of the pointwise correlation of each topology metric (Table I) shows that  $\lambda_C$  is very nearly linearly related to  $v_E$ , similar to the simple example above. Both the FTLE and  $\Theta$  showed positive correlations with  $v_E$ , but root-mean-square errors of both were an order of magnitude greater than that of  $\lambda_C$ , demonstrating the robustness of  $\lambda_C$  as a surrogate

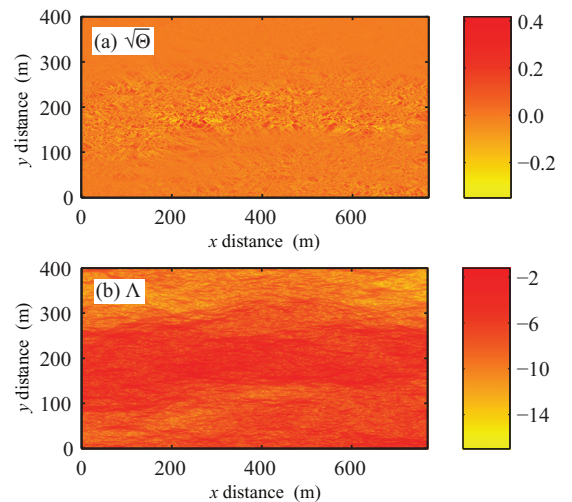


FIG. 2. (Color online) (a) Square root of the Okubo-Weiss parameter  $\sqrt{\Theta}$  and (b) finite-time Lyapunov exponent. The complex nature of the velocity field causes significant noise in  $\Theta$ .



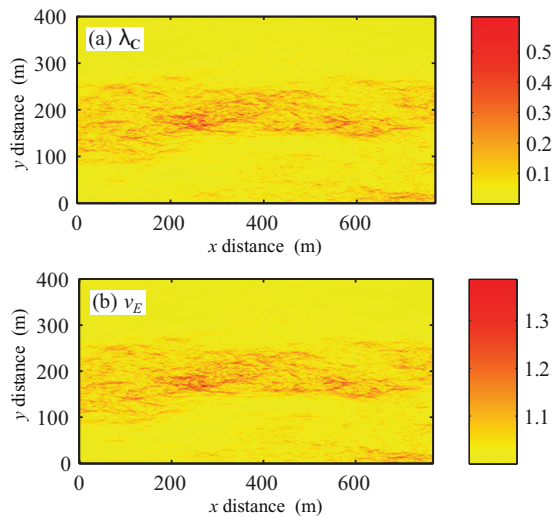


FIG. 3. (Color online) (a) Largest eigenvalue of the Cauchy-Green tensor  $\lambda_C$  and (b) relative enhancement of the CLD  $\nu_E(\mathbf{s})$ . The areas with the highest changes in CLD are predicted very accurately from  $\lambda_C$  (Table I).

for CLD and thus best for informing mixing and reaction rates.

**Discussion.** Flow deformation metrics have a clear link to mixing-limited reactive transport. The nearly identical patterns of  $\lambda_C$  and the CLD enhancement (Fig. 3) show precisely where the highest reaction rates within the domain are likely to occur, assuming a mixing-limited reaction. Actual reaction rates will depend on the initial conditions of the reactants and their transport properties, so it is necessary to consider changes in CLD conditional to these factors, but the CLD conditional to a specific problem cannot exceed the unconditional CLD [i.e., Fig. 3(b)] and is thus an end member of the problem.

Neither the Okubo-Weiss parameter nor the FTLE, while clearly able to qualitatively capture the behavior, produces an ideal map of the enhanced CLD. The Okubo-Weiss parameter overemphasizes rotation, a factor that does not contribute to mixing and reaction. The logarithmic scaling of the FTLE penalizes higher values of  $\lambda_C$ . Another analytic example of the Okubo-Weiss parameter poorly reflecting reaction is in a shear flow with  $E_{11} = E_{22} = E_{12} = 0$  and  $E_{21} = \sigma/2$ , which must increase the reactions by changing particle proximity (and dispersion variance) but for which

TABLE I. Summary statistics of the linear regression of the correlation of  $\Theta$ , FTLE, and  $\lambda_C$  to the actual CLD; RMSE is root-mean-square error and SSE is the sum of squared errors.

Metric	$R^2$	RMSE	SSE
$\Theta$	0.68	$4.90 \times 10^{-2}$	740.70
FTLE	0.95	$1.76 \times 10^{-2}$	94.89
$\lambda_C$	0.99	$1.80 \times 10^{-3}$	1.03

$\Theta = 0$ . However, it is noteworthy that both  $\Theta(\mathbf{x})$  and  $\Lambda(\mathbf{x})$  give good predictions of the regions where the CLD does not change where the flow is relatively uniform. Deformation metrics based on the Cauchy-Green tensor are less sensitive to the complex velocity field because they are rotationally invariant to the reference frame [35]. In other words, they represent Lagrangian deformations, which is precisely why they relate so well to changes in CLD, which are also purely Lagrangian. The mathematical relationship for this more general case can be shown for small  $\Delta t$ , when  $\nu_E \approx 1 + s_0^2 \Delta t \lambda_c^2 / 8 D_m$ . For rotation-free flow,  $\lambda_c^2 = \lambda_C / \Delta t^2$  and the reaction rate potential remains approximately linear with the largest eigenvalue of the Cauchy-Green tensor, as reflected in Fig. 3. Note that while we have chosen to work with the (right) Cauchy-Green tensor, we could also have chosen to work with another common symmetric and rotationless metric, the (left) Cauchy-Green tensor, and obtained the same results as the eigenvalues of both Cauchy-Green tensors are the same. We chose to work with the (right) Cauchy-Green tensor due to its widespread use across disciplines [35].

This Rapid Communication highlights three main points about mixing and reactions. First, the framework for simulating mixing and reactions provided by collocation probabilities avoids difficulties presented by concentration-based mixing measures and maintains a direct connection to the underlying physics of reactions as stochastic processes. Second, changes in collocation relative to a purely diffusive case represent an unconditional map of the maximum possible reaction rates within the domain and these areas can be accurately inferred directly from the velocity field. Finally, we show that the largest eigenvalue of the Cauchy-Green tensor is approximately linear with the relative CLD, which clearly shows that the areas of highest enhanced reaction potential occur where the nonrotational deformations are the strongest. These ideas, while directly relevant to fluid systems, are applicable to any reactive system with heterogeneous flows.

- [1] J. Allam, M. T. Sajjad, R. Sutton, K. Litvinenko, Z. Wang, S. Siddique, Q.-H. Yang, W. H. Loh, and T. Brown, *Phys. Rev. Lett.* **111**, 197401 (2013).
- [2] A. M. Tartakovsky, D. M. Tartakovsky, and P. Meakin, *Phys. Rev. Lett.* **101**, 044502 (2008).
- [3] S. Rüdiger, J. W. Shuai, and I. M. Sokolov, *Phys. Rev. Lett.* **105**, 048103 (2010).
- [4] J. Seinfeld and S. Pandis, *Atmospheric Chemistry and Physics: From Air Pollution to Climate Change* (Wiley, New York, 2006).
- [5] F. Bartumeus, J. Catalan, U. L. Fulco, M. L. Lyra, and G. M. Viswanathan, *Phys. Rev. Lett.* **88**, 097901 (2002).
- [6] J. Murray, *Mathematical Biology: I. An Introduction*, Vol. 2 (Springer, Berlin, 2002).
- [7] J. Knebel, T. Krüger, M. F. Weber, and E. Frey, *Phys. Rev. Lett.* **110**, 168106 (2013).
- [8] J. Fort and V. Méndez, *Phys. Rev. E* **60**, 5894 (1999).
- [9] D. Becherer and M. Schweizer, *Ann. Appl. Probab.* **15**, 1111 (2005).

- [10] F. Schweitzer, *Brownian Agents and Active Particles: Collective Dynamics in the Natural and Social Sciences* (Springer, Berlin, 2007).
- [11] E. Kotomin and V. Kuzovkov, *Modern Aspects of Diffusion-Controlled Reactions: Cooperative Phenomena in Bimolecular Processes* (Elsevier, Amsterdam, 1996).
- [12] O. Bénichou, C. Chevalier, J. Klafter, B. Meyer, and R. Voituriez, *Nat. Chem.* **2**, 472 (2010).
- [13] E. Monson and R. Kopelman, *Phys. Rev. Lett.* **85**, 666 (2000).
- [14] S. Atis, S. Saha, H. Auradou, D. Salin, and L. Talon, *Phys. Rev. Lett.* **110**, 148301 (2013).
- [15] C. M. Gramling, C. F. Harvey, and L. C. Meigs, *Environ. Sci. Technol.* **36**, 2508 (2002).
- [16] P. K. Kitanidis, *Water Resour. Res.* **30**, 2011 (1994).
- [17] T. Le Borgne, M. Dentz, D. Bolster, J. Carrera, J.-R. De Dreuzy, and P. Davy, *Adv. Water Resour.* **33**, 1468 (2010).
- [18] B. Jha, L. Cueto-Felgueroso, and R. Juanes, *Phys. Rev. Lett.* **106**, 194502 (2011).
- [19] J. J. Hidalgo, J. Fe, L. Cueto-Felgueroso, and R. Juanes, *Phys. Rev. Lett.* **109**, 264503 (2012).
- [20] E. Villiermaux and J. Duplat, *Phys. Rev. Lett.* **91**, 184501 (2003).
- [21] T. Le Borgne, M. Dentz, and E. Villiermaux, *Phys. Rev. Lett.* **110**, 204501 (2013).
- [22] E. Castro-Alcala, D. Fernandez-Garcia, J. Carrera, and D. Bolster, *Environ. Sci. Technol.* **46**, 3228 (2012).
- [23] T. Le Borgne, M. Dentz, P. Davy, D. Bolster, J. Carrera, J.-R. de Dreuzy, and O. Bour, *Phys. Rev. E* **84**, 015301 (2011).
- [24] M. Lévy, in *Coherent Vortices and Tracer Transport*, edited by A. Provenzale, A. Babiano, A. Bracco, C. Pasquero, and J. B. Weiss, Lecture Notes in Physics Vol. 744 (Springer, Berlin, 2008), pp. 219–261.
- [25] D. Toussaint and F. Wilczek, *J. Chem. Phys.* **78**, 2642 (1983).
- [26] D. Gillespie, *J. Chem. Phys.* **113**, 297 (2000).
- [27] J. S. van Zon and P. R. ten Wolde, *Phys. Rev. Lett.* **94**, 128103 (2005).
- [28] D. A. Benson and M. M. Meerschaert, *Water Resour. Res.* **44**, W12201 (2008).
- [29] A. Paster, D. Bolster, and D. Benson, *J. Comput. Phys.* **263**, 91 (2014).
- [30] A. Paster, D. Bolster, and D. A. Benson, *Water Resour. Res.* **49**, 1 (2013).
- [31] D. Ding, D. A. Benson, A. Paster, and D. Bolster, *Adv. Water Resour.* **53**, 56 (2013).
- [32] H. Tennekes and J. L. Lumley, *A First Course in Turbulence* (MIT Press, Cambridge, 1972).
- [33] F. P. J. de Barros, M. Dentz, J. Kock, and W. Nowak, *Geophys. Res. Lett.* **39**, L08404 (2012).
- [34] D. Bolster, P. de Anna, D. A. Benson, and A. M. Tartakovsky, *Adv. Water Resour.* **37**, 86 (2012).
- [35] T. Peacock and G. Haller, *Phys. Today* **66** (2), 41 (2013).
- [36] G. Haller, *Physica D* **240**, 574 (2011).
- [37] D. R. Lester, G. Metcalfe, and M. G. Trefry, *Phys. Rev. Lett.* **111**, 174101 (2013).